Detailed velocity model building in a carbonate karst zone and improving sub-karst images in the Gulf of Mexico

Jun Cai*, Hao Xun, Li Li, Yang He, Zhiming Li, Shuqian Dong, Manhong Guo and Bin Wang, TGS

Summary

A velocity anomaly zone with high contrasts and small wavelength variations is often a challenge for conventional depth imaging. It requires model details that are usually smoothed out because of the noise present in the data. In the eastern Gulf of Mexico, carbonate karst zones are often found over the Florida Escarpment as shown in Figure 1. The karst zones have significantly slower velocities than the surrounding sediments. The size of these karsts is usually a few meters to a few hundred meters. The resulting seismic images below the karst zones are often poor and non-geological (Figure 2). A synthetic modeling study has been conducted to give more insight into the difficulty of running conventional tomography, and to provide some guidelines for modeling the karst zone velocity anomaly. A new velocity model building technique has been developed that combines karst modeling and horizon-driven tomography. The geological information and interpretation are used as input as well as constraints to seismic tomography. The integration of geological interpretation and seismic tomography enable us to derive a detailed velocity model and improve the seismic image in the area.
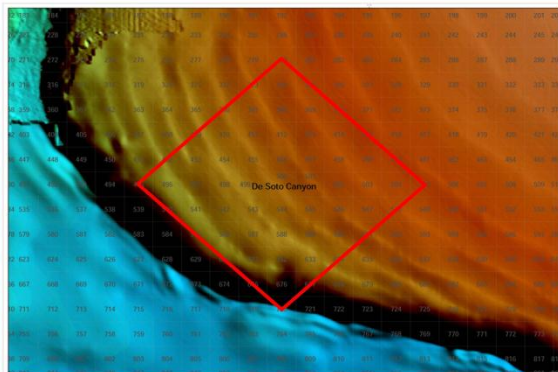
Figure 1: Study area in the eastern Gulf Mexico.

Introduction

Karst within the parent carbonate rock presents a great challenge to accurately map sub-karst prospects and adequately plan well paths. Correctly identifying and mapping the karst structures could provide useful information, not only for reserve estimation, but also to avoid potential drilling hazards. The seismic velocity of unconsolidated sediments associated with karst features is usually significantly lower than the carbonate parent rock, making it possible to identify such zones on seismic data. However, the spatial locations and the sizes and the shapes of these karsts are very irregular, making the detailed modeling of the karst zones a challenging task, especially using the PreStack Depth Migration (PSDM) stacks.
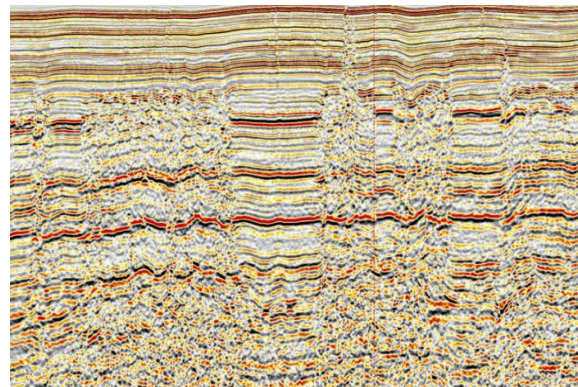

Figure 2: Without correct karst velocity model, the sub-karst images are often poor and non-geological.

In order to map a karst feature, the velocity model building becomes a critical step. Two potential conventional approaches are depth domain reflection tomography, which flattens the migrated Common Image Gathers (CIGs); and full waveform inversion, which adjusts the velocity model to match the amplitude differences between the synthetic forward modeling and observed field data.

The presence of karst features causes a noisy zone below the karst. The lack of clear events makes the tomography input CIG picking very difficult. The karst features are often localized and contradict the normal tomography assumption that the initial background velocity is smooth. From the synthetic study, we learned that there are more fundamental challenges for conventional reflection tomography, which will be discussed later. Full waveform inversion, constrained by the inaccuracy of the density description, usually only uses the refracted wave, which has limited penetration depth. For the study area, most of the karst zones are below 2.5 km, which is deeper than a refracted wave received by the acquisition. However, for near surface karst imaging, there has been some success using refraction tomography (Sheehan et al., 2005). Similar to full waveform inversion, refraction tomography is also limited by the refraction depth. In this paper, we present a new technique, which combines modeling the low velocity karst zone with horizon driven tomography to build the velocity model.

Synthetic Study

In order to get more insight into the problem, a finite difference modeling program with input reflectivity and velocity model (Biondi, 2006) was used to generate a synthetic dataset. Figure 3A shows the true velocity model, which has a smooth vertical gradient with various low velocity anomalies. The low velocity anomalies are meant to simulate the karst features. Horizontal reflectivity boundaries are generated at 300 m intervals (Figure 3F) and are used to generate the reflection events.

Next, we migrated the synthetic data using only the smooth background velocity without the low velocity details, to simulate the effects on the migration image by using a smooth velocity model. Figure 3B shows the CIGs around the low velocity spot on the far left. From the CIGs we can see there are some fundamental challenges for a conventional tomography solution, besides the potential difficulties listed in the introduction section. In conventional tomography, we normally assume that the near offset always has less velocity error than the middle and far offsets. In turn, in the CIGs, the near offset events are used as a reference to flatten the gathers. In Figure 3B, we can see that because of the size of the velocity anomalies, the impact of the low velocity is localized. In turn, right underneath the low velocity areas, the near offsets have more depth error than other offsets, which is contrary to conventional tomography assumptions. If tomography uses the near offset events as a reference to flatten the middle and far offsets, it will derive a faster velocity instead of the low velocity that was modeled. During the tomography picking process, we need to describe the residual move-out by some type of analytical formula; Figure 3B shows it is going to be difficult to find a simple parabolic or hyperbolic curve to describe the move-out beneath the low velocity anomalies. From this study, we found that some novel approaches to solve the problem are required.

One possible solution is to use the migration stack response as an indication of velocity changes. Figure 3C shows the full migration stack for a smooth background velocity. From Figure 3C, we can see that the "waviness" of events below the low velocity zones depends on the size of the low velocity zones. For the two small low velocity anomalies on the right, the local low velocity impacts are healed quickly. The two larger low-velocity anomalies on the left have an impact on the image even at greater depths. Only reflectors close to the low velocity anomalies give a clear indication of the low velocity. It is more interesting to see the low velocity responses for different offset ranges.
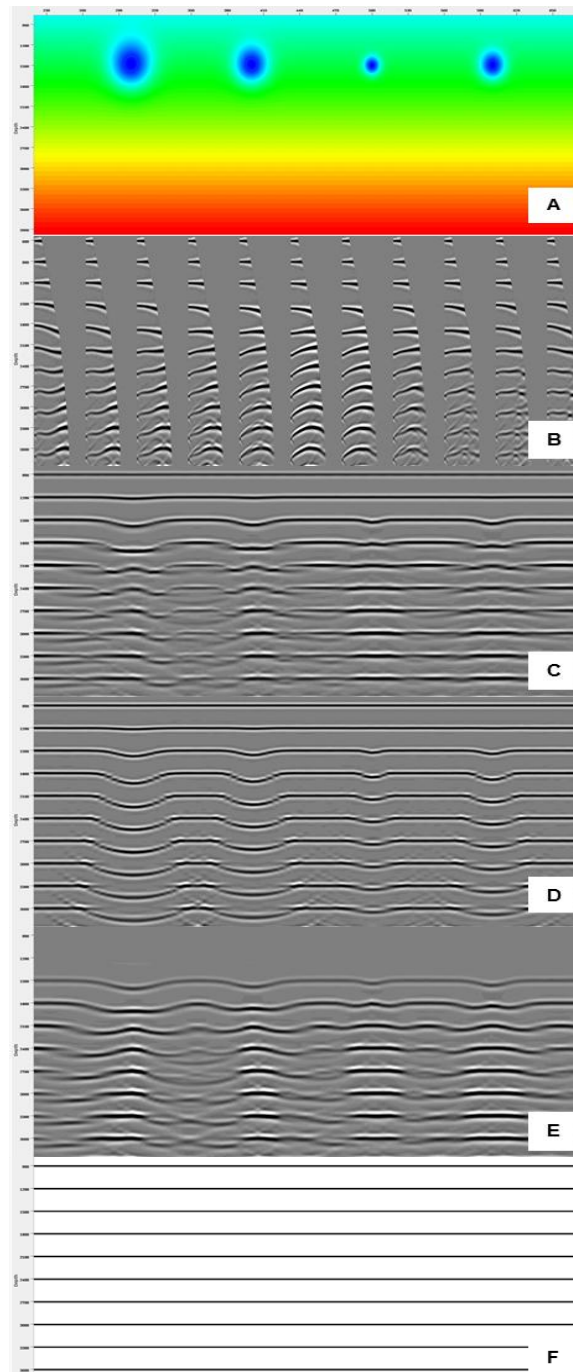

Figure 3: Synthetic examples. (A) True velocity model for synthetic data. Migration results for smooth background velocity: (B)CIGs around the low velocity anomaly on far left; (C) full stack; (D) near offset stack; (E) far offset stack. Three stacks (C-E) show very different images. (F) true reflectivity model.

Detailed karst velocity model building

Figures 3D and 3E are a migration of a near offset stack, and a far offset stack, respectively. All three stacks (full, near and far offsets) are very different from the true image (Figure 3F). Clearly, the near offset stack (Figure 3D) gives the most consistent indication of the low velocity anomalies. Consequently, the near offset PSDM stack is used for horizon interpretation in the field data example.

Technique and field data examples

As a result of the synthetic study, we developed a workflow as shown in Figure 4. First, conventional high resolution tomography was used to build an accurate velocity model above the karst zone; followed by a depth migration to generate a near offset stack (Figure 5).
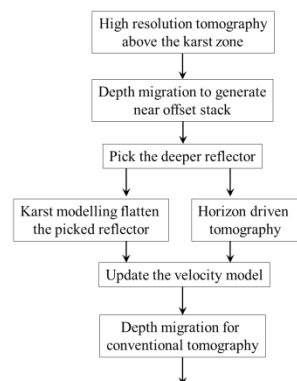

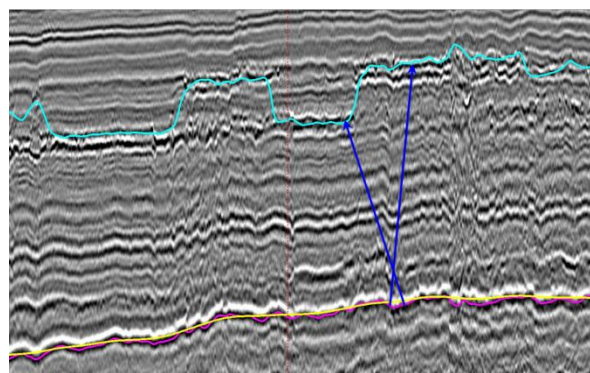Figure 4: Karst velocity model building flow.

Figure 5: Near offset stack as input for karst modeling and horizon driven tomography.

From the PSDM near offset stack (Figure 5), we can see the start of low S/N images below the light blue horizon, indicating the start of the karst zone. The "waviness" of the seismic images can be seen below the karst zone, narrow in the shallow section and broader in the deep section - very similar to what the synthetic study predicts. However, in this region, geological information indicates the sub-karst

zone reflector layers should be relatively smooth. For example in Figure 5, the picked magenta reflector should be close to the target surface in yellow. The fluctuations within the noisy zone are caused by the velocity model errors in the shallow corresponding to the karst feature. The starting depth for the velocity update is determined by the picked surface shown in light blue. Since the karst should be closely related to the starting point of the noisy area, 3D coherent attributes were calculated to help pick the starting depth for the low velocity anomalies corresponding to karst areas.

For the karst modeling, the near offset stack is de-migrated to the time domain first using the current migration velocity. The 20% lower local velocity anomalies are added to the current velocity model to build the new model. Next post-stack migration using the updated velocity model is conducted to check the depth correction for the current magenta surface. These procedures are performed iteratively by adjusting the thickness of the low velocity anomalies, until the picked current magenta surface migrates to the target yellow surface.

To improve the convergence speed of the subsequent regular tomography, a new horizon driven tomography was developed. For each location the horizon driven tomography shoots a ray perpendicular to the current magenta surface (blue arrows in Figure 5); the travel time error for this ray is calculated between the current magenta surface and the target yellow surface. The velocity updates are limited to between the picked top surface (in light blue) and the current surface (in magenta).

The velocity model derived from karst modeling and the model derived from horizon driven tomography have been combined to build a velocity model that can be used as input to additional tomography for further improvements. Figure 6 shows the velocity model before (Figure 6A) and after (Figure 6B) karst modeling and horizon driven tomography. The karst modeling derived a slow velocity karst feature with a vertical size smaller than 400 m. The karsts are scattered within a narrow depth range. Horizon driven tomography derived velocity variations between the top surface and current surface. The combined velocity model (Figure 6B) dramatically improves the sub-karst migration in the near offset stacks (Figure 6D). The sub-karst reflectors are more coherent (Figure 6D) compared to the previous migration near offset stack (Figure 6C). This indicates a better initial model has been created as input to the subsequent tomography to further refine the velocity model. A benefit from the RTM's ability to handle sharp velocity contrasts is improvement in the continuity of the sub-karst zone (Figure 7), in turn RTM could be a better tool for detail karst velocity model building.

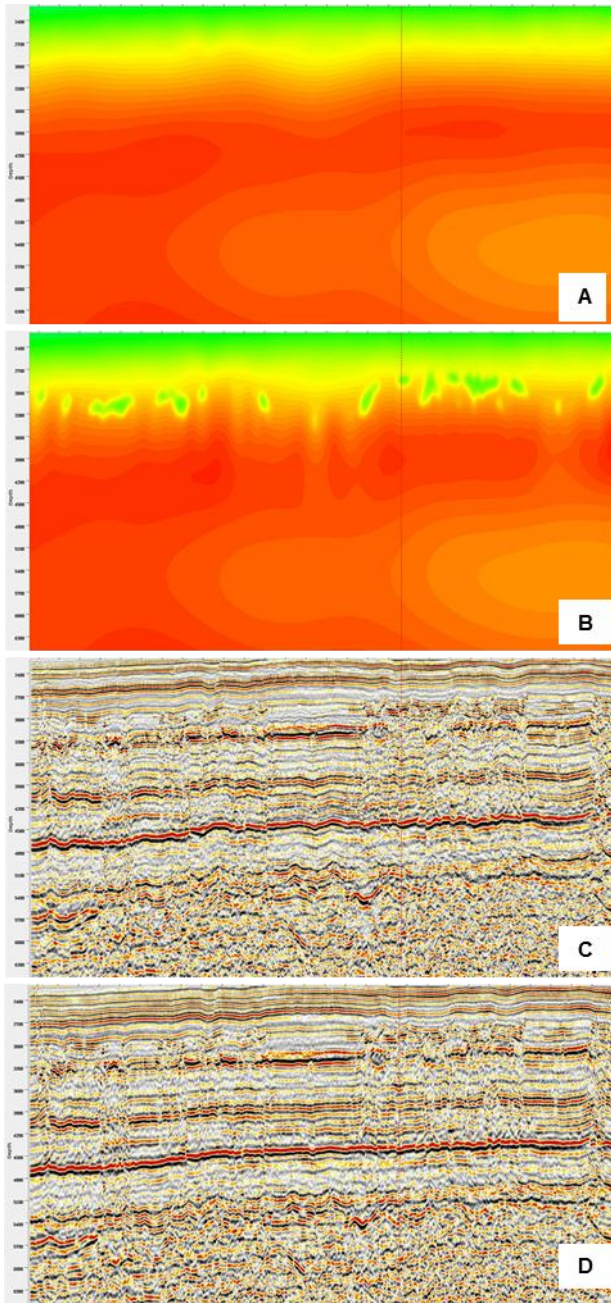# Detailed karst velocity model building

Figure 6: Velocity model update and corresponding near offset stack responses. (A) Velocity models before (A) and after (B) karst modeling and horizon driven tomography. (C) Migration near offset stack using velocity model shown in (A). (D) Migration near offset stack using updated velocity model shown in (B).
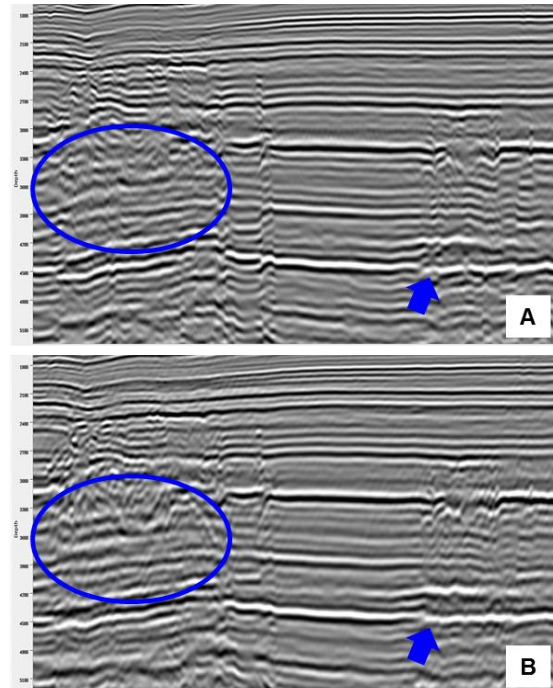

Figure 7: RTM further improves the continuity for sub-karst zone. (A): Kirchhoff migration image. (B) RTM migration image.

Conclusions

Our synthetic experiment gave us insight into how the low velocity karst impacts both CIGs and the migration stack. A new technique of karst modeling and horizon driven tomography has been developed. The geological information and interpretation are used in these new technologies. Field data examples showed that the velocity update from karst modeling and horizon driven tomography gave a great uplift to the images of the pre-stack depth migration. The updated velocity model paves the way for the subsequent conventional tomography update around and below the karst areas.

Acknowledgments

The authors would like to thank David Prouty, ZhongYang Dong, Gary Rodriguez, George Cloudy Jr., Quincy Zhang and Itze Chang for their valuable contributions during the project. We thank the management of TGS for permission to publish this paper. The authors also thank Laurie Geiger and Simon Baldock for proof reading.

EDITED REFERENCES
Note: This reference list is a copy-edited version of the reference list submitted by the author. Reference lists for the 2011 SEG Technical Program Expanded Abstracts have been copy edited so that references provided with the online metadata for each paper will achieve a high degree of linking to cited sources that appear on the Web.

REFERENCES

Biondi, B., 2006, Prestack exploding-reflectors modeling for migration velocity analysis: 76th Annual International Meeting, SEG, Expanded Abstracts, **25**, 3056–3060.

Sheehan, J. R., W. E. Doll, D. B. Watson, and W. A. Mandell, 2005, Application of seismic refraction tomography to karst cavities: U. S. Geological Survey Karst Interest Group.

Proceedings, R. C., and S. Dakota, 2005, U. S. Geological Survey Scientific Investigations Report 2005-5160.